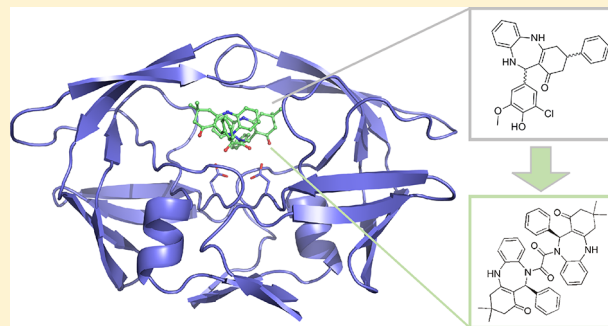


## Structure-Aided Design of Novel Inhibitors of HIV Protease Based on a Benzodiazepine Scaffold

Jiří Schimer,<sup>†,‡</sup> Petr Cígler,<sup>†</sup> Jan Veselý,<sup>§</sup> Klára Grantz Šašková,<sup>†</sup> Martin Lepšík,<sup>†</sup> Jiří Brynda,<sup>†,||</sup> Pavlína Řezáčová,<sup>†,||</sup> Milan Kožíšek,<sup>†</sup> Ivana Císařová,<sup>¶</sup> Heike Oberwinkler,<sup>⊥</sup> Hans-Georg Kraeusslich,<sup>⊥</sup> and Jan Konvalinka<sup>\*,†,‡</sup><sup>†</sup>Institute of Organic Chemistry and Biochemistry, Gilead Sciences and IOCB Research Center, Academy of Sciences of the Czech Republic, Flemingovo n. 2, 166 10, Prague 6, Czech Republic<sup>‡</sup>Department of Biochemistry, <sup>§</sup>Department of Organic Chemistry, and <sup>¶</sup>Department of Inorganic Chemistry, Faculty of Science, Charles University, Hlavova 8, 128 43, Prague 2, Czech Republic<sup>||</sup>Institute of Molecular Genetics, Academy of Sciences of the Czech Republic, Vídeňská 1083, Prague 4, Czech Republic<sup>⊥</sup>Department of Infectious Diseases, Virology, Heidelberg University, Im Neuenheimer Feld 324, 69120 Heidelberg, Germany

## Supporting Information

**ABSTRACT:** HIV protease is a primary target for the design of virostatics. Screening of libraries of non-peptide low molecular weight compounds led to the identification of several new compounds that inhibit HIV PR in the low micromolar range. X-ray structure of the complex of one of them, a dibenzo[*b,e*][1,4]-diazepinone derivative, showed that two molecules of the inhibitor bind to the PR active site. Covalent linkage of two molecules of such a compound by a two-carbon linker led to a decrease of the inhibition constant of the resulting compound by 3 orders of magnitude. Molecular modeling shows that these dimeric inhibitors form two crucial hydrogen bonds to the catalytic aspartates that are responsible for their improved activity compared to the monomeric parental building blocks. Dibenzo[*b,e*][1,4]-diazepinone analogues might represent a potential new class of HIV PIs.



## INTRODUCTION

More than 25 years after its discovery, HIV protease (HIV PR) remains one of the primary targets for development of novel HIV treatments. Because HIV PR plays a key role in the life cycle of the virus, its inhibition prevents maturation of the viral particles and renders them noninfectious.<sup>1</sup> Protease inhibitors (PIs), combined with other antiretroviral drugs in “highly active antiretroviral therapy” (HAART), can decrease viral load below measurable levels and greatly increase the life expectancy and quality of life of HIV patients. However, the high cost of HAART, the occurrence of various side effects, and the emergence of highly mutated viral strains cross-resistant to antiretrovirals have motivated both academic researchers and the pharmaceutical industry to develop novel PIs. These second generation PIs exhibit improved pharmacokinetic properties, fewer side effects, and a more favorable activity profile against highly resistant viral species than their predecessors.<sup>2</sup> Development of HIV PIs remains one of the most remarkable examples of structure-aided drug design and a test case for novel approaches in medicinal chemistry (for review see refs 3 and 4).

In the past decade, the U.S. Food and Drug Administration (FDA) has approved several highly effective second generation PIs, including darunavir, that exhibit a low picomolar  $K_i$  and

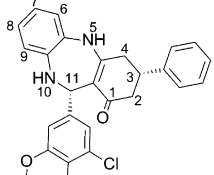
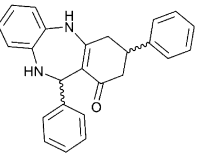
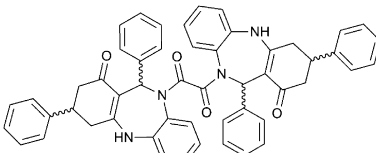
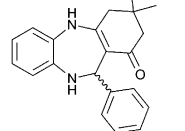
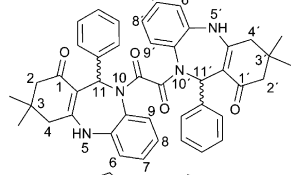
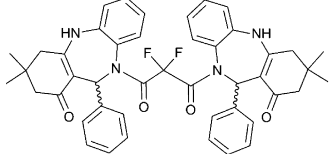
favorable resistance profile.<sup>5</sup> A number of other PIs have been recently reported. We searched for novel structures that might adopt an alternative binding mode to HIV PR and thus possibly exhibit a different resistance profile than current PIs. As a result, we and others identified several unexpected chemical structures that have been reported to inhibit HIV PR. These compounds include fullerenes, niobium-based polyoxometalates, and icosahedral carboranes (for a recent review of new PIs, see ref 6). The need for new structural types that open alternative pathways for rational drug design, however, remains urgent.

Recently, our laboratory screened a variety of chemical structures for inhibition of HIV replication. This led to the identification of several new compounds that inhibit HIV PR in the low micromolar range. One of these compounds is a dibenzo[*b,e*][1,4]-diazepinone derivative (compound 1, Table 1). 1,4-Benzodiazepines have been widely used as psychoactive compounds since the mid-1960s. In the past two decades, benzodiazepines experienced a renaissance period during which high throughput screening panels containing various diazepine analogues were applied to various enzymatic targets. These

Received: August 29, 2012

Published: October 11, 2012

**Table 1. Diazepine-Based Inhibitors of HIV-1 PR and Their In Vitro Inhibitory Activity toward HIV-1 PR**

Compound No.	Structure	Molecular weight	IC <sub>50</sub> [μM]
1		446.14	4.3 <sup>a</sup>
2		366.17	20 <sup>a</sup>
3		786.32	0.06 <sup>b</sup>
4		318.17	110 <sup>a</sup>
5		690.32	0.03 <sup>b</sup>
6		740.31	0.3 <sup>a</sup>

<sup>a</sup>IC<sub>50</sub> of diastereomeric mixture was determined. <sup>b</sup>IC<sub>50</sub> of more active diastereomer (11*R*,11'*R* and 11*S*,11'*S*) was determined.

screens led to identification of several potential drugs, some of which were recently approved for clinical use (for a review of diazepines, see ref 7). Because benzodiazepines are considered an excellent pharmacophore owing to their nontoxicity and good pharmacokinetic properties, **1** was selected for further development by structure-aided drug design.

## RESULTS

Compound **1** (Table 1) is a low micromolar (IC<sub>50</sub> of 4.3 μM) inhibitor of HIV PR. Kinetic analysis showed that **1** is not purely competitive (Supporting Information). Nevertheless, X-ray crystallography of the corresponding complex with HIV PR showed that the inhibitor does bind to the PR active site. Interestingly, two molecules of **1** were found in the PR binding cleft (Figure 1).

The two molecules of **1** bind symmetrically into the C2 symmetric protease dimer with semiopen flaps covering the active site. The inhibitor molecules occupy the active site of the enzyme but do not directly interact with the catalytic aspartates. They make numerous van der Waals interactions with flap residues Ile47, Gly48, and Leu50 and residues 80–84, which

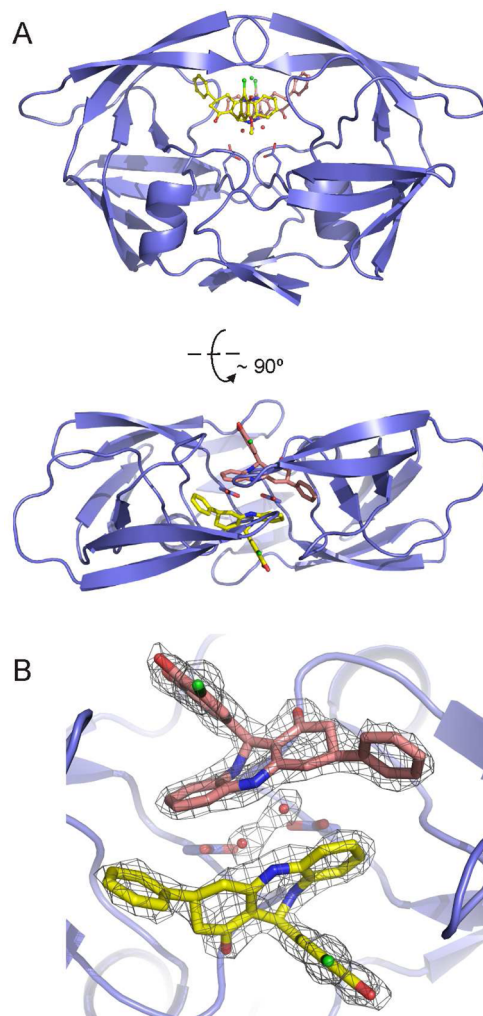


**Figure 1.** Crystal structure of wild-type HIV PR in complex with compound **1**. (A) Two views of the overall structure. The protein is shown in cartoon representation with the catalytic aspartates shown in stick representation. Two copies of **1** bound to the active site are shown in stick representation. Carbon atoms are shown in pink and yellow to distinguish the two molecules. Oxygen, nitrogen, and chlorine atoms are colored red, blue, and green, respectively. Structural water molecules and chloride ion are shown as red and green spheres, respectively. (B) Detailed top view of the enzyme active site. The electron density map ( $2F_o - F_c$  map contoured at  $1.5\sigma$  level) for the two molecules of **1** and water molecules W1 and W2 is shown in gray. Flap residues covering the active site are omitted for clarity. Stereoview version of Figure 1 is shown in Supporting Information.

belong to the S3 and S3' substrate binding pockets (Figure 2A). The only polar interaction between inhibitor and enzyme is between imino group N21 of **1** and the main-chain carbonyl oxygen of Gly 27. Additional interactions are mediated through water molecules located at the bottom of the active site and through a chloride anion located under the tips of the flaps. Water molecules (designated W1 and W2 in the crystal structure) make hydrogen bonds with the side chains of the catalytic aspartates and are within hydrogen-bonding distance of N21 of compound **1**. A chloride ion located between the inhibitor and enzyme flaps bridges the imino groups of Ile50 in both chains and N14 of compound **1** through four acceptor hydrogen bonds. This interaction is analogous to that of the so-called flap water molecule present in crystal structures of HIV PR in complex with peptidomimetic inhibitors.<sup>4</sup> The

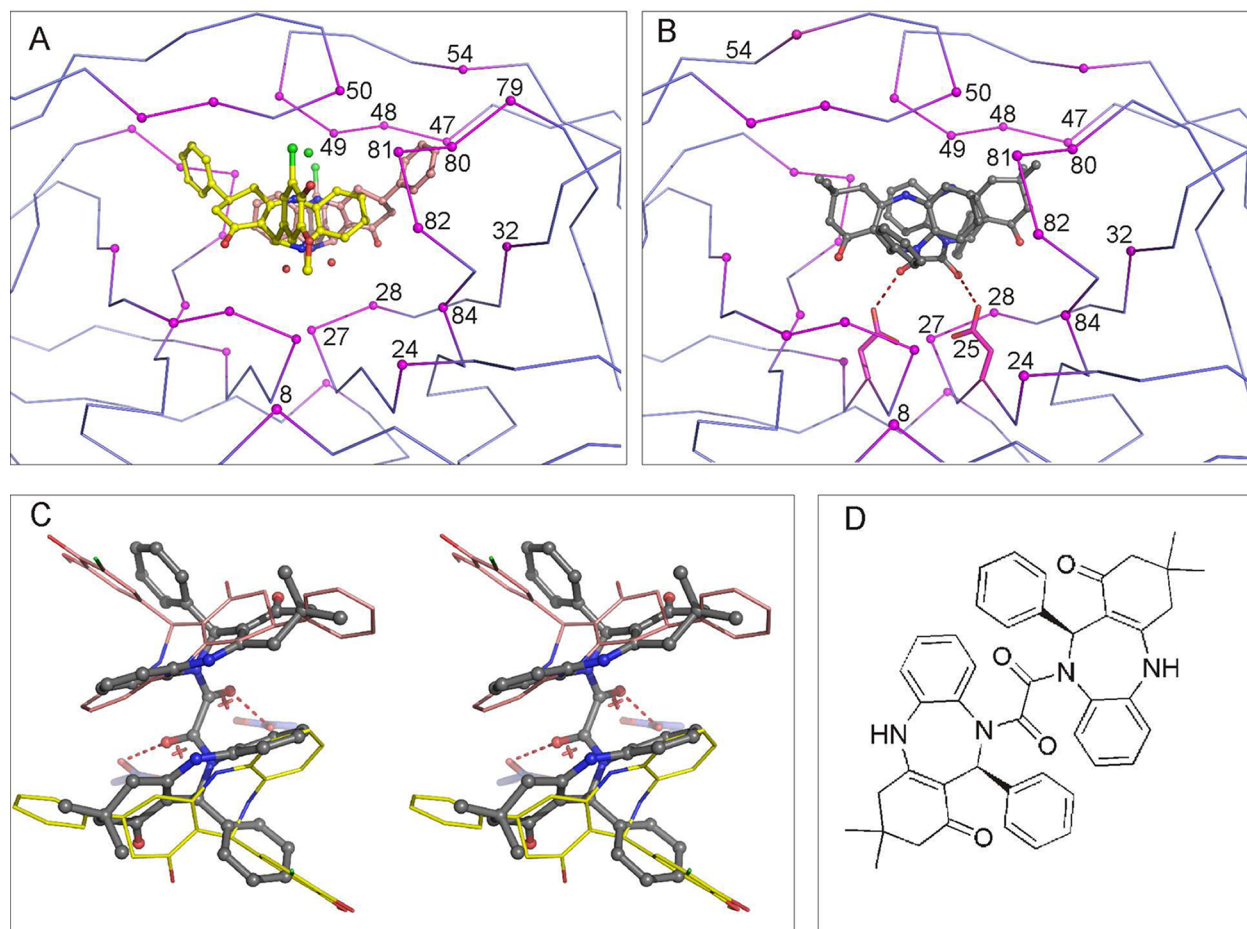


**Figure 2.** (A) Interaction of compound **1** in the active site of HIV PR in the crystal structure.  $C\alpha$  atoms of residues in contact with the inhibitor are depicted as spheres and colored magenta (residue numbering is indicated only for one protein chain). A detailed list of interactions is summarized in Supporting Information Table S2. (B) Interaction of compound **5a** (11*S*,11'*S* configuration) in the active site of HIV PR in the model. Residues in contact with inhibitor are highlighted by their  $C\alpha$  atoms and colored magenta. Polar contacts with catalytic aspartates are shown as red dashed lines (the hydrogen-bonding distances between protein and inhibitor oxygens are 2.6 Å). (C) Superposition of the binding modes of compounds **1** and **5**. Stereoview of the active site corresponds to bottom panel of Figure 1. For clarity, the protein chain is not shown and catalytic aspartates are represented by sticks. Two structural water molecules present in the crystal structure are represented by red crosses. (D) Structural formula of the single enantiomer of compound **5a** (11*S*,11'*S*) which fitted into the active site cavity based on docking (cf. Figure 3).

replacement of the flap water by a properly positioned oxygen atom from an inhibitor molecule has often been used to improve the binding of non-peptide inhibitors of HIV PR (for recent examples, see refs 25 and 26)

Binding of two molecules of **1** to the active site suggests that linking the molecules might lead to more favorable binding to the PR binding cleft. There are examples of this in the literature, observed with both HIV PR and other proteins, as well as a theoretical explanation of this phenomenon.<sup>27</sup> Two molecules of a derivative of **1** (**2**, Table 1) were connected by a two-carbon linker (oxalyl), mainly for synthetic simplicity. The resulting inhibitor (**3**, Table 1) showed an inhibition constant lower than that of the monomeric **2** by more than 2 orders of magnitude.

Compounds lacking the phenyl moieties attached to carbons 11 and 11' (**7** and **8**) showed moderate decreases in inhibitory activity and decreased solubility.

The most potent inhibitor (**5a**) is selective for HIV PR. It inhibits neither the related aspartic protease human cathepsin D nor papain, a prototype cysteine protease (see Supporting Information for details).

Molecular docking suggested that only one enantiomer of **5** would fit into the active site of HIV PR for steric reasons (Figure 2D). The docked conformation of **5a** showed an occupation of the active site similar to the two molecules of **1**. Notably, the positions of the two carbonyl oxygens of the linker nearly coincided with the positions of the two water molecules found in the X-ray structure of the HIV PR–**1** complex (cf. Figure 2A,B). Thus, the carbonyl oxygens of **5a** were positioned appropriately to form two hydrogen bonds with the enzyme's catalytic aspartates (Figure 2B).

A comparison of the docked structure of **5a** in HIV PR with the X-ray structure of the HIV PR–**1** complex shows that the two dibenzodiazepine cores occupy similar positions in the enzyme binding pocket, but because of the short oxalyl linker, those of **5** are closer to each other and adopt an almost parallel mutual orientation (Figure 2C). While the two cores occupy the S3–S2' enzyme subsites in a unique arrangement, their substituents (the phenyl moieties attached to C3 in **1**) point to previously unexplored parts of the binding site. Interestingly, the two structural water molecules, W1 and W2, which are within hydrogen-bonding distances of the outer O $\delta$  atoms of Asp25 and Asp25' (2.82 and 2.59 Å, respectively), nearly

perfectly coincide with the two oxalyl oxygens of **5a** (Figure 2C).

## DISCUSSION

Here, we report the identification of dibenzo[*b,e*][1,4]-diazepinones as a new class of HIV PIs. As shown by the X-ray structure, two molecules of the parental compound (**1**) bind to the PR active cleft in a unique mode. By joining two molecules of the weakly inhibiting **1**, we obtained dimeric compounds that bind over 2 orders of magnitude more favorably, thus confirming general theoretical predictions.<sup>28</sup>

Despite extensive efforts, our attempts to obtain the crystal structure of **5a** in complex with HIV PR were not successful. We therefore employed molecular modeling to suggest a possible structure (Figure 2B). The greatly enhanced inhibitory ability of dimeric inhibitor **5a** compared to monomeric inhibitor **4** may be explained in part by thermodynamics. The entropic contribution of only a single molecule in the active center of HIV PR is lower than that of two molecules (as in the case of the monomeric inhibitor). Furthermore, two key hydrogen bonds that are formed between the catalytic aspartates and two oxygens from the oxalyl group of **5a** (Figure 2) contribute to the improved binding. The lack of these crucial hydrogen bonds might explain the decreased activity of **6** (Table 1) compared to **5a**. In the case of **6**, a diastereomeric mixture was tested for inhibition of HIV PR (the ratio of diastereomers was 2.5:1). However, even if the less abundant diastereomer was the only active one, the inhibitory activity of **6** is still lower than that of **5a**.

The only structural difference between **5a** and **5b** (Table 2) is the relative configuration of phenyl groups connected to

carbons 11 and 11'. Multidimensional NMR analyses combined with molecular modeling suggested that the absolute configuration of **5a** is 11*R*,11'*R*, and 11*S*,11'*S* (i.e., **5a** is a mixture of two enantiomers) while **5b** is the 11*S*,11'*R* enantiomer. These configurations were confirmed by X-ray analysis. This finding is similar to the results of the crystallographic analysis conducted on **2** (the crystal was grown from a diastereomeric mixture, and both active diastereomers were present in the crystal). The isolated diastereomers of **2** differ only in the configuration of phenyl groups connected to carbon 3, and the phenyl groups at carbon 11 are in the same configuration as in **5a**. A significant drop in inhibitory activity is observed when the phenyl groups are removed (compare the  $IC_{50}$  values for **7** and **8** with that for **5a**). Thus, we can conclude that the phenyl groups and their relative configurations play a crucial role in the activity of this novel class of inhibitors.

The docking of the substituted dimeric variants allowed us to identify the enantiomers that could favorably fit into the binding pocket (see Figure 3). Thus, for example, the 3-order-

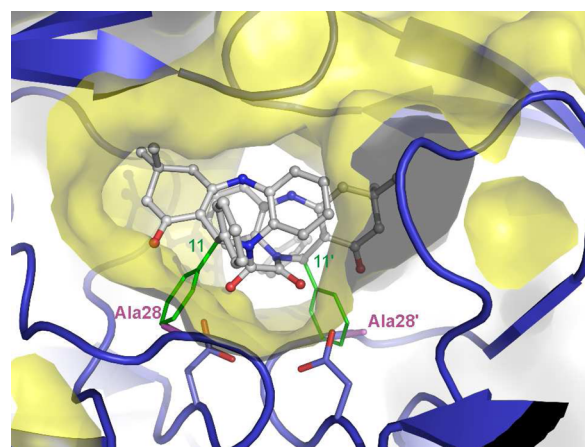


**Figure 3.** Compound **5** (in sticks) docked into the active site of HIV-1 PR (blue protein with yellow surface). A single enantiomer of compound **5a** (the two phenyls in the 11*S*,11'*S* configuration) fitted into the cavity, while the second enantiomer (with 11*R*,11'*R* configuration) depicted in green sticks showed serious steric clashes with the area of the active site around Ala28/28' (side chain depicted in magenta).

**Table 2. Relationship between Relative Configuration and Inhibitor Activity for Dimers of **1****

Compound No.	R <sub>1</sub> =R <sub>2</sub>	Absolute configuration	IC <sub>50</sub>
5a		11 <i>R</i> , 11' <i>R</i> ; 11 <i>S</i> , 11' <i>S</i>	30 nM <sup>a</sup>
5b		11 <i>R</i> , 11' <i>S</i>	> 1 μM
7		—	200 nM
-----			
8		11 <i>R</i> ; 11 <i>S</i>	100 nM <sup>a</sup>

<sup>a</sup>IC<sub>50</sub> of enantiomeric mixture was determined.

of-magnitude difference in affinity between **5a** and **5b** (Table 2) may be due (Figure 3) to steric clashes of 11/11' phenyls with PR residues (mostly Ala28/28').

In summary, we have shown that dibenzo[*b,e*][1,4]-diazepinone analogues are a potential new class of HIV PIs, with apparent  $K_i$  values as low as 12 nM. We used X-ray structure analysis combined with molecular modeling to show that dimeric inhibitors form two crucial hydrogen bonds to catalytic aspartates. This is likely the most important feature of their improved activity compared to the monomeric parental building blocks.

## EXPERIMENTAL SECTION

Compound libraries and screening will be described elsewhere.

**Chemical Synthesis. Instrument Techniques.** <sup>1</sup>H, <sup>13</sup>C, and <sup>19</sup>F NMR spectroscopy was performed with three different instruments: Varian UNITY-Inova 300 MHz, Bruker Avance 600 MHz, and Bruker Avance 500 MHz. Chemical shifts are shown in ppm, and coupling constants are shown in Hz. To fully verify the structure of inhibitors,

two-dimensional NMR spectroscopy was employed, including HSQC, HMBC, COSY, and ROESY (measured with the Bruker Avance 600 MHz instrument). High resolution mass spectrometry measurements were performed on LTQ Orbitrap XL instrument (Thermo Fisher Scientific) using electrospray ionization. Positive ions were detected. Solvents and reagents were used as purchased from Sigma Aldrich (U.S.) with the exception of dry THF, which was purchased from Acros Chemicals (Belgium). Crystallographic data were collected on three different instruments (for details, see Supporting Information). The purity of all compounds was determined by elemental analysis and met the criteria for  $\geq 95\%$  purity (except for compounds **6** and **7**; for details see Supporting Information). An automated CHN analyzer (PE 2400 series II CHNS/O analyzer) was used for determination of C, H, N elemental composition. For determination of Cl, the X-ray fluorescence method (SPECTRO iQII spectrometer) was employed.

**General Procedure for Preparation of Dimeric Inhibitors (Example of Synthesis and Spectral Data Shown for Compound 5).** In a round-bottom flask compound **4** (1.500 g, 4.71 mmol) and Et<sub>3</sub>N (1.017 g, 10.8 mmol) were dissolved in dry THF (30 mL) under argon atmosphere and cooled to  $-43\text{ }^{\circ}\text{C}$ . Oxalyl chloride (0.299 g, 2.36 mmol) was slowly added dropwise (0.299 g added in 1.5 h) to the stirring solution under argon atmosphere. The rate at which the oxalyl chloride is added determines which diastereomer is formed (faster rate results in formation of enantiomer with 11R,11'S configuration only). After 10 min, the mixture was left to warm up to room temperature and stirred for further 1 h. The reaction was then quenched by addition of 30 mL of EtOAc. The organic phase was washed with 0.1 M HCl (25 mL) and twice with water ( $2 \times 25\text{ mL}$ ). White precipitate in the organic phase was then filtered yielding a mixture of diastereomers **5a** and **5b** in moderate yield (600 mg, 37%). The two diastereomers were separated using preparative TLC (Merck, TLC silica gel 60 F<sub>254</sub>, 2 mm); the mobile phase was DCM/MeOH (19:1).

Bis(3,3-dimethyl-11-phenyl-2,3,4,5,10,11-hexahydro-1H-dibenzo-[b,c][1,4]diazepin-1-one-10-yl) oxalate (compound **5a**, mixture of enantiomers 11R,11'R and 11S,11'S) was prepared as described in the general procedure (600 mg, 37% for mixture of diastereomers). <sup>1</sup>H NMR (500 MHz, DMSO):  $\delta$  8.23 (bs, 2H), 7.13–7.10 (m, 2H), 7.10 (s, 2H), 7.09–7.05 (m, 4H), 7.02–6.98 (m, 4H), 6.80–6.77 (m, 4H), 6.67 (bt, 2H,  $J = 7.3\text{ Hz}$ ), 6.67–6.65 (m, 2H), 2.35 (d, 2H,  $J = 16.8\text{ Hz}$ ), 2.19 (d, 2H,  $J = 16.8\text{ Hz}$ ), 2.04 (d, 2H,  $J = 15.6\text{ Hz}$ ), 2.02 (d, 2H,  $J = 15.6\text{ Hz}$ ), 1.03 (s, 6H), 0.99 (s, 6H). <sup>13</sup>C NMR (125 MHz, DMSO):  $\delta$  192.41, 162.77, 153.09, 139.20, 137.09, 129.32, 127.83 (overlap), 127.28, 126.80, 126.72, 121.96, 120.45, 106.34, 53.72, 49.36, 43.81, 31.32, 29.32, 26.70. Calculated monoisotopic mass: 691.3279. HRMS ESI<sup>+</sup> found: 691.3280. Calculated elemental composition (%): C 76.50, H 6.13, N 8.11. Found: C 74.04, H 6.06, N 7.81.

**Enzymes.** The expression, refolding, and purification of HIV PR were performed as previously described.<sup>8</sup> Human cathepsin D, kindly provided by Michael Mares (Institute of Organic Chemistry and Biochemistry, Academy of Sciences of the Czech Republic), was isolated from human placenta as previously described.<sup>9</sup> Papain was purchased from Sigma (St. Louis, MO, U.S.).

**Inhibition Assays.** For inhibition of HIV PR, both IC<sub>50</sub> and K<sub>i</sub> values were determined by spectrophotometric assay using the chromogenic substrate KARVNIeNphEANle-NH<sub>2</sub>, as previously described.<sup>10</sup> The mechanisms of inhibition were determined using Lineweaver–Burk plots.

For inhibition of cathepsin D and papain, a spectrofluorometry assay in a microplate setup was used to determine the possible inhibitory activity of compound **5a**. The enzymes (0.7 nM) were preincubated with various concentrations of **5a** in 0.1 M sodium acetate, pH 4.8, containing up to 2.5% DMSO, for 1 min at 37 °C. The reaction was started by adding substrate (Abz-KPAEFF\*AL, 6.3 mM; Abz represents chromogenic *o*-aminobenzoic acid, and the asterisk indicates the cleavage site) prepared by Fmoc solid phase peptide synthesis. The product release was continuously monitored using excitation and emission wavelengths of 330 and 410 nm, respectively, with a GENios Plus instrument (Tecan Group Ltd., Switzerland).<sup>9</sup>

**Crystallization, Data Collection, and Structure Solution.** The HIV PR–**1** complex was prepared by mixing the enzyme with a 5-fold

molar excess of the inhibitor dissolved in DMSO, followed by concentration to 5 mg/mL by ultrafiltration using Microcon-10 filters (Millipore, Billerica, MA, U.S.). Crystals were grown by the hanging drop vapor diffusion technique at 19 °C. The crystallization drops contained 2  $\mu\text{L}$  of protein–inhibitor complex and 1  $\mu\text{L}$  of reservoir solution (0.7 M NaCl and 0.1 M MES, pH 6.5). For diffraction measurements, crystals were soaked in reservoir solution supplemented with 25% (v/v) glycerol and cryocooled in liquid nitrogen.

X-ray diffraction data were collected at 120 K on a Mar345 image plate system using a Nonius FR591 rotating anode generator. Diffraction data were integrated and reduced using MOSFLM<sup>11</sup> and scaled using SCALA<sup>12</sup> from the CCP4 suite.<sup>13</sup> Crystal parameters and data collection statistics are given in Table S1.

The crystal structure was determined by molecular replacement using the program Molrep<sup>14</sup> with the structure of HIV PR (PDB code 1U8G,<sup>15</sup>) as a template. Model refinement was carried out using the program REFMAC 5.5.0109<sup>16</sup> from the CCP4 package,<sup>13</sup> interspersed with manual adjustments using Coot.<sup>17</sup> The final steps included TLS refinement.<sup>18</sup> The quality of the final models was validated with Molprobit.<sup>19</sup> All figures showing structural representations were prepared with the program PyMOL.<sup>20</sup> The electron density used for modeling of **1** into the enzyme active site was of excellent quality. Considering the abundance of chloride ion in crystallization buffer as well as the chemical environment in the structure (namely, the presence of four hydrogen bond donor groups in the vicinity), the spherical electron density map observed under the tip of flaps was explained by the presence of a chloride anion.

Final refinement statistics are given in Table S1. Atomic coordinates and experimental structure factors have been deposited in the Protein Data Bank with the code 3T11 (<http://www.pdb.org>).

**Molecular Modeling.** Docking of all the enantiomers of compound **5** into HIV PR was performed using DOCK 6.2.<sup>21</sup> The crystal structure of HIV PR in complex with **1** (PDB code 3T11, this work) was used as a starting structure. The protein was prepared by removing the ligands, waters, and ions and by adding hydrogens. All the enantiomers of **5** were constructed starting from the X-ray structure of **5a** (Figure S2, this work). Hydrogens were added, and GAFF parameters<sup>22</sup> and AM1-BCC charges<sup>23</sup> were assigned using Chimera 1.5.3.<sup>24</sup> The chiral center inversion was done in PyMOL.<sup>19</sup> The binding site was defined by spheres extending to 2 Å from **1** in the HIV PR complex X-ray structure. A grid across the binding site was generated with default parameters except that an all-atom model was used. Rigid docking was thereafter performed with default settings except that the maximum number of ligand orientations was increased to 1500 and the maximum number of minimization iterations was set to 2500.

## ■ ASSOCIATED CONTENT

### 📄 Supporting Information

Synthesis of remaining inhibitors, further characterization of all compounds (<sup>1</sup>H and <sup>13</sup>C NMR, high resolution mass spectrometry), X-ray characterization of individual inhibitors and HIV PR complex with compound **1** (list of all contacts between HIV PR and compound **1**), kinetic analysis of HIV PR inhibition by compound **1**, and inhibition study of cathepsin and papain with compound **5a**; a separate file containing stereoview of Figure 1. This material is available free of charge via the Internet at <http://pubs.acs.org>.

## ■ AUTHOR INFORMATION

### Corresponding Author

\*Phone: +420-220183218. Fax: +420-220183578. E-mail: [konval@uochb.cas.cz](mailto:konval@uochb.cas.cz).

### Notes

The authors declare no competing financial interest.

## ACKNOWLEDGMENTS

The authors thank Hillary Hoffman for critical proofreading of the manuscript and the Grant Agency of the Czech Republic (Program P208/12/G016 and Grant P/207/11/1798) for funding. This work was also in part supported by research projects AV0Z40550506, and AV0Z50520514 awarded by the Academy of Sciences of the Czech Republic.

## ABBREVIATIONS USED

HIV PR, human immunodeficiency virus protease; PI, protease inhibitor; HAART, highly active antiretroviral therapy; FDA, Food and Drug Administration

## REFERENCES

- (1) Kohl, N. E.; Emini, E. A.; Schleif, W. A.; Davis, L. J.; Heimbach, J. C.; Dixon, R. A.; Scolnick, E. M.; Sigal, I. S. Active human immunodeficiency virus protease is required for viral infectivity. *Proc. Natl. Acad. Sci. U.S.A.* **1988**, *85* (13), 4686–4690.
- (2) Wensing, A. M.; van Maarseveen, N. M.; Nijhuis, M. Fifteen years of HIV protease inhibitors: raising the barrier to resistance. *Antiviral Res.* **2010**, *85* (1), 59–74.
- (3) Menendez-Arias, L. Molecular basis of human immunodeficiency virus drug resistance: an update. *Antiviral Res.* **2010**, *85* (1), 210–231.
- (4) Wlodawer, A.; Vondrasek, J. Inhibitors of HIV-1 protease: a major success of structure-assisted drug design. *Annu. Rev. Biophys. Biomol. Struct.* **1998**, *27*, 249–284.
- (5) Koh, Y.; Nakata, H.; Maeda, K.; Ogata, H.; Bilcer, G.; Devasamudram, T.; Kincaid, J. F.; Boross, P.; Wang, Y. F.; Tie, Y.; Volarath, P.; Gaddis, L.; Harrison, R. W.; Weber, I. T.; Ghosh, A. K.; Mitsuya, H. Novel bis-tetrahydrofuranylethane-containing non-peptidic protease inhibitor (PI) UIC-94017 (TMC114) with potent activity against multi-PI-resistant human immunodeficiency virus in vitro. *Antimicrob. Agents Chemother.* **2003**, *47* (10), 3123–3129.
- (6) Pokorna, J.; Machala, L.; Rezacova, P.; Konvalinka, J. Current and novel inhibitors of HIV protease. *Viruses* **2009**, *1* (3), 1209–1239.
- (7) Ramajayam, R.; Giridhar, R.; Yadav, M. R. Current scenario of 1,4-diazepines as potent biomolecules—a mini review. *Mini-Rev. Med. Chem.* **2007**, *7* (8), 793–812.
- (8) Saskova, K. G.; Kozisek, M.; Lepsik, M.; Brynda, J.; Rezacova, P.; Vaclavikova, J.; Kagan, R. M.; Machala, L.; Konvalinka, J. Enzymatic and structural analysis of the I47A mutation contributing to the reduced susceptibility to HIV protease inhibitor lopinavir. *Protein Sci.* **2008**, *17* (9), 1555–1564.
- (9) Masa, M.; Maresova, L.; Vondrasek, J.; Horn, M.; Jezek, J.; Mares, M. Cathepsin D propeptide: mechanism and regulation of its interaction with the catalytic core. *Biochemistry* **2006**, *45* (51), 15474–15482.
- (10) Richards, A. D.; Phylip, L. H.; Farmerie, W. G.; Scarborough, P. E.; Alvarez, A.; Dunn, B. M.; Hirel, P. H.; Konvalinka, J.; Strop, P.; Pavlickova, L.; et al. Sensitive, soluble chromogenic substrates for HIV-1 proteinase. *J. Biol. Chem.* **1990**, *265* (14), 7733–7736.
- (11) Leslie, A. G. Integration of macromolecular diffraction data. *Acta Crystallogr., Sect. D: Biol. Crystallogr.* **1999**, *55* (Part 10), 1696–1702.
- (12) Evans, P. R. Data Reduction. In *Proceedings of CCP4 Study Weekend on Data Collection and Processing*; Daresbury Laboratory: Warrington, U.K., 1993; pp 114–122.
- (13) The CCP4 suite: programs for protein crystallography. *Acta Crystallogr., Sect. D: Biol. Crystallogr.* **1994**, *50* (Part 5), 760–763.
- (14) Vagin, A.; Teplyakov, A. An approach to multi-copy search in molecular replacement. *Acta Crystallogr., Sect. D: Biol. Crystallogr.* **2000**, *56* (Part 12), 1622–1624.
- (15) Brynda, J.; Rezacova, P.; Fabry, M.; Horejsi, M.; Stouracova, R.; Soucek, M.; Hradilek, M.; Konvalinka, J.; Sedlacek, J. Inhibitor binding at the protein interface in crystals of a HIV-1 protease complex. *Acta Crystallogr., Sect. D: Biol. Crystallogr.* **2004**, *60* (Part 11), 1943–1948.
- (16) Murshudov, G. N.; Vagin, A. A.; Dodson, E. J. Refinement of macromolecular structures by the maximum-likelihood method. *Acta Crystallogr., Sect. D: Biol. Crystallogr.* **1997**, *53* (Part 3), 240–255.
- (17) Emsley, P.; Cowtan, K. Coot: model-building tools for molecular graphics. *Acta Crystallogr., Sect. D: Biol. Crystallogr.* **2004**, *60* (Part 12, Part 1), 2126–2132.
- (18) Winn, M. D.; Isupov, M. N.; Murshudov, G. N. Use of TLS parameters to model anisotropic displacements in macromolecular refinement. *Acta Crystallogr., Sect. D: Biol. Crystallogr.* **2001**, *57* (Part 1), 122–133.
- (19) Lovell, S. C.; Davis, I. W.; Arendall, W. B., 3rd; de Bakker, P. I.; Word, J. M.; Prisant, M. G.; Richardson, J. S.; Richardson, D. C. Structure validation by Alpha geometry: phi, psi and Cbeta deviation. *Proteins* **2003**, *50* (3), 437–450.
- (20) DeLano, W. L. *The PyMOL Molecular Graphics System*; DeLano Scientific LLC: San Carlos, CA; <http://www.pymol.org>.
- (21) Lang, P. T.; Brozell, S. R.; Mukherjee, S.; Pettersen, E. F.; Meng, E. C.; Thomas, V.; Rizzo, R. C.; Case, D. A.; James, T. L.; Kuntz, I. D. DOCK 6: combining techniques to model RNA-small molecule complexes. *RNA* **2009**, *15* (6), 1219–1230.
- (22) Wang, J.; Wolf, R. M.; Caldwell, J. W.; Kollman, P. A.; Case, D. A. Development and testing of a general Amber force field. *J. Comput. Chem.* **2004**, *25* (9), 1157–1174.
- (23) Jakalian, A.; Jack, D. B.; Bayly, C. I. Fast, efficient generation of high-quality atomic charges. AM1-BCC model: II. Parameterization and validation. *J. Comput. Chem.* **2002**, *23* (16), 1623–1641.
- (24) Pettersen, E. F.; Goddard, T. D.; Huang, C. C.; Couch, G. S.; Greenblatt, D. M.; Meng, E. C.; Ferrin, T. E. UCSF Chimera—a visualization system for exploratory research and analysis. *J. Comput. Chem.* **2004**, *25* (13), 1605–1612.
- (25) Hodge, C. N.; Aldrich, P. E.; Bacheler, L. T.; Chang, C. H.; Eyermann, C. J.; Garber, S.; Grubb, M.; Jackson, D. A.; Jadhav, P. K.; Korant, B.; Lam, P. Y.; Maurin, M. B.; Meek, J. L.; Otto, M. J.; Rayner, M. M.; Reid, C.; Sharpe, T. R.; Shum, L.; Winslow, D. L.; Erickson-Viitanen, S. Improved cyclic urea inhibitors of the HIV-1 protease: synthesis, potency, resistance profile, human pharmacokinetics and X-ray crystal structure of DMP 450. *Chem. Biol.* **1996**, *3* (4), 301–314.
- (26) Muzammil, S.; Armstrong, A. A.; Kang, L. W.; Jakalian, A.; Bonneau, P. R.; Schmelmer, V.; Amzel, L. M.; Freire, E. Unique thermodynamic response of tipranavir to human immunodeficiency virus type 1 protease drug resistance mutations. *J. Virol.* **2007**, *81* (10), 5144–5154.
- (27) Specker, E.; Bottcher, J.; Lilie, H.; Heine, A.; Schoop, A.; Muller, G.; Griebenow, N.; Klebe, G. An old target revisited: two new privileged skeletons and an unexpected binding mode for HIV-protease inhibitors. *Angew. Chem., Int. Ed.* **2005**, *44* (20), 3140–3144.
- (28) Zhou, H. X.; Gilson, M. K. Theory of free energy and entropy in noncovalent binding. *Chem. Rev.* **2009**, *109* (9), 4092–4107.